OPEN ACCESS Freely available online

PLoS PATHOGENS

The Fittest versus the Flattest: Experimental Confirmation of the Quasispecies Effect with Subviral Pathogens

Francisco M. Codoñer[1], José-Antonio Daròs[1], Ricard V. Solé[2,3], Santiago F. Elena[1*]

1 Instituto de Biología Molecular y Celular de Plantas, Consejo Superior de Investigaciones Científicas–Universitat Politècnica de València, València, Spain, **2** Complex Systems Laboratory, Institució Catalana de Recerca i Estudis Avançats-Universitat Pompeu Fabra, Barcelona, Spain, **3** Santa Fe Institute, Santa Fe, New Mexico, United States of America

The "survival of the fittest" is the paradigm of Darwinian evolution in which the best-adapted replicators are favored by natural selection. However, at high mutation rates, the fittest organisms are not necessarily the fastest replicators but rather are those that show the greatest robustness against deleterious mutational effects, even at the cost of a low replication rate. This scenario, dubbed the "survival of the flattest", has so far only been shown to operate in digital organisms. We show that "survival of the flattest" can also occur in biological entities by analyzing the outcome of competition between two viroid species coinfecting the same plant. Under optimal growth conditions, a viroid species characterized by fast population growth and genetic homogeneity outcompeted a viroid species with slow population growth and a high degree of variation. In contrast, the slow-growth species was able to outcompete the fast species when the mutation rate was increased. These experimental results were supported by an in silico model of competing viroid quasispecies.

Citation: Codoñer FM, Daròs JA, Solé RV, Elena SF (2006) The fittest versus the flattest: Experimental confirmation of the quasispecies effect with subviral pathogens. PLoS Pathog 2(12): e136. doi:10.1371/journal.ppat.0020136

Introduction

The two most basic processes of evolution are mutation and selection. In the simplest Darwinian paradigm, natural selection acts on existing genetic variation and favors those genotypes with the higher fitness. High fitness is usually, but not always, associated with fast replication, but when the mutation rate is so high that each newly generated individual carries genetic defects, fitness can also be maximized by reducing the impact of these mutations on an individual's phenotype. Therefore, the selective advantage of genetically robust systems is their decreased susceptibility to deleterious mutations, regardless of their replication rate. Whether robustness (i.e., the reduced sensitivity of phenotypes to perturbations) is an evolved property or is intrinsic to genetic systems is largely unknown, because the mechanistic basis for robustness would depend on the peculiarities of each system. One of the simplest situations in which mutational robustness evolves at the population level is represented by the quasispecies model of molecular evolution [1–4]. According to this model, selection would maximize the average replication rate of the swarm of genotypes interconnected by mutation rather than favoring the genotype with the highest replication rate [1–4]. Hence, mutation acts as a selective agent and shapes the genome in a manner that causes the entire quasispecies to become robust against mutations. Thus, in a highly mutagenic environment, a quasispecies occupying a low but flat region in the fitness landscape should outcompete a quasispecies located at a higher but narrower fitness peak when most of its surrounding mutants are unfit [4–6]. This phenomenon has been called the quasispecies effect or, more recently, the "survival of the flattest" in clear reference to Darwin's "survival of the fittest" [7,8].

Despite the attractiveness of the survival of the flattest, empirical evidence directly supporting this theory has so far been restricted to the work of Wilke et al. with digital organisms [7] and of Wilke in simulated RNA evolution [9]. Here, we use an experimental system very well-suited for testing the applicability of the hypothesis to biological entities: two viroid species that infect the same host. Viroids are subviral plant pathogens whose genomes are composed of a small (246–401 nucleotides long) single-stranded circular RNA molecule that does not encode any protein but is able to replicate in susceptible host plants [10,11]. A very structured and characteristic RNA folding pattern represents the only "phenotype" of viroids. Rod-like structures are typical for the family Pospiviroidae, whereas more branched structures are typical for the family Avsunviroidae.

Twenty-five of the 29 known viroid species belong to the family Pospiviroidae (named after *Potato spindle tuber viroid*, the type species of the family). All of them contain a central conserved region, and depending on the degree of similarity within this region, members of the family are assigned to five different genera. Pospiviroidae replicate and accumulate in

Editor: Raul Andino, University of California San Francisco, United States of America

Received July 20, 2006; **Accepted** November 14, 2006; **Published** December 29, 2006

Abbreviations: CChMVd, *Chrysanthemum chlorotic mottle avsunviroid;* CSVd, *Chrysanthemum stunt pospiviroid;* SEM, standard error of the mean; UVC, ultraviolet C light

* To whom correspondence should be addressed. E-mail: sfelena@ibmcp.upv.es

Synopsis

Darwin's "survival of the fittest" suggests that faster replicators are able to outcompete slower ones. However, when mutation, unavoidably associated with genome replication, is incorporated into the picture, the situation becomes a bit more complicated. At a high mutation rate, being the faster replicator may not always be the best option; in fact, being the more robust against the pernicious effect of mutation may be a better option. If a tradeoff exists between mutational robustness and replication rate—for example, because faster polymerases are more prone to mistakes than slower ones—then selection may favor an organism to replicate faster or to be more robust, but not both at the same time. At a low mutation rate, a faster replicator would displace a robust one. However, beyond a critical mutation rate, the slower replicator should outcompete the faster replicator. This phenomenon is known as the "survival of the flattest". Here, the authors have confirmed this prediction using a pair of subviral plant pathogens (viroids) competing under normal and mutagenic conditions.

the nucleus [10,11]. The other four known viroids form the family Avsunviroidae (named after *Avocado sunblotch viroid*, the type species of the family). Avsunviroidae lack the characteristic structural motifs of the Pospiviroidae and contain hammerhead ribozymes. Apart from the common hammerhead structures, sequence similarities among Avsunviroidae are remarkably low. Avsunviroidae replicate and accumulate in chloroplasts [10,11]. Although viroids require cellular factors to complete their infectious cycle, Avsunviroidae exhibit ribozyme activities that self-process multimeric replicative intermediates [10].

The two viroid species chosen for this study were *Chrysanthemum stunt pospiviroid* (CSVd) [12] and *Chrysanthemum chlorotic mottle avsunviroid* (CChMVd) [13]. This choice was made based upon four biological properties. (i) In plants initially inoculated with equivalent amounts of each viroid and for which systemic infection was established for an extended period, the concentration of CChMVd per gram of fresh plant tissue was ~20 times lower than for CSVd (Table 1), suggesting a lower net population growth rate for CChMVd. (ii) In contrast, the genetic variability of the CChMVd quasispecies was much larger than for the CSVd quasispecies by all indexes examined (Table 1). (iii) Both viroid species invade the whole plant, and the presence of several Avsunviroidae and Pospiviroidae in the same cell types of infected leaves has been confirmed by in situ hybridization experiments [14–16], thus creating conditions that allow intracellular competition for resources. (iv) In silico, the neutral neighborhood (i.e., the fraction of all possible one-error mutants, including deletions, that do not change the minimum free energy secondary structure) for the CChMVd molecule is ~2 times larger than for the CSVd molecule [17–19] (Table 1). Consistent with this, sequencing of multiple clones of both viroids from systemically infected plants revealed that CChMVd quasispecies were composed of molecules more diverse in folding stability (ratio of standard deviations for minimum free energies: 3.234) and shape [20] (ratio of standard deviations for differences in shape: 27.462) than CSVd quasispecies (Table 1). Therefore, CChMVd quasispecies grow slowly, are genetically heterogeneous, and exhibit a remarkable diversity of RNA secondary structures. In contrast, CSVd quasispecies grow rapidly and are genetically and structurally homogeneous. According to the survival of the flattest effect, CSVd should outcompete CChMVd at low mutation rates, whereas CChMVd should be superior at high mutation rates.

Results/Discussion

Increasing the Mutation Rate Affects the Outcome of the Competition between CSVd and CChMVd

To directly test the survival-of-the-flattest phenomenon, chrysanthemum plants (*Dendranthema grandiflora* Tzvelev. cv "Bonnie Jean") were grafted with scions taken from donor plants singly infected with CChMVd or CSVd. Then, 2 wk after grafting, the presence of both viroids was confirmed by Northern blot analysis. Forty-two cuttings from a coinfected plant were planted into individual pots. After rooting, half of the plants were moved into a growth chamber (24 °C and a 16-h light period) and the other half were moved into a second chamber (same growth conditions) in which they were irradiated 10 min/d with an ultraviolet C light (UVC) germicidal lamp (Phillips G36T8; maximal output at 253.7 nm; dose 2 J/cm^2). The negative impact of UVC radiation on the in vivo replication and accumulation of RNA viruses (e.g., [21–23]) and viroids [24] has been known for several decades. UVC irradiation of RNA results in a variety of products, including uridine photohydrates and pyrimidine photodimers [25,26]. Uridine photohydrates may block translation but also miscode for cytidine during the synthesis of progeny RNA [27]. Molecules carrying pyrimidine cyclobutane photodimers between adjacent residues or cross-linked nonadjacent residues produce abortive RNA synthesis when used as templates. In addition, UVC radiation generates reactive oxygen species that may produce more than 35 different base modifications [28]. The UVC daily dose used in this experiment was in the same order of magnitude as that required for inducing in vitro and in vivo intramolecular cross-linking in viroids from both families [29,30], while still minimizing its effect on the growth of the host plants.

The first set of plants represents the control for competition under normal (low mutation rate) environmental conditions, whereas the second represents the competition under environment-induced mutagenic conditions. Two ($n = 3$), four ($n = 6$), and six ($n = 12$) weeks after initiation of the experiment, n plants from each treatment regime were taken and the proportion of both viroids in each sample was estimated by quantitative Northern blot using ^{32}P-labeled-specific riboprobes. Figure 1 shows that a UVC-induced increase in mutation rate affects the outcome of the competition between CChMVd and CSVd (t-test, $p = 0.002$). Under unmanipulated (i.e., low mutation rate) conditions, the median ratio CChMVd:CSVd significantly decreased as CSVd outcompeted CChMVd (t-test, $p = 0.011$). The negative slope of the log regression on the median values, –0.086 ± 0.019, represents a measure of the selective disadvantage of CChMVd relative to CSVd. This ~9% per week selective disadvantage can easily be explained as a consequence of CChMVd's slower growth rate, and is in excellent agreement with the Darwinian survival-of-the-fittest paradigm. In contrast, when the mutation rate was artificially increased by UVC, the competition was completely different, and the faster replicator CSVd was no longer able to outcompete the more robust replicator CChMVd, as predicted by the survival-

Table 1. Replication, Diversity, and Robustness Characteristics of CChMVd and CSVd Quasispecies

Property		CChMVd (Dataset S1, $n = 8$) ($\pm$ SEM)	CSVd (Dataset S4, $n = 11$) ($\pm$ SEM)	Ratio CChMVd:CSVd
Growth	RNA accumulation (arbitrary units per gram of fresh plant tissue)	8,082	154,119	0.05
Diversity	Haplotype diversity (percent)	100 $\pm$ 2	93 $\pm$ 2	1.08
	Average number of nucleotide differences	7.7 $\pm$ 0.1	2.47 $\pm$ 0.03	3.12
Robustness	Size of neutral neighborhood (percent)	15.73 $\pm$ 0.01	7.51 $\pm$ 0.01	2.09
	Average deviation from the optimum free energy[a] (kcal/mol at 37 °C)	4 $\pm$ 1	1.2 $\pm$ 0.3	3.33
	Average deviation from the optimum secondary structure shape[b]	81 $\pm$ 34	3 $\pm$ 1	27

The variance in the magnitude of the deviation was significantly larger for CChMVd than for CSVd.
[a]Levene's test, $p < 0.001$.
[b]Levene's test, $p = 0.001$.
doi:10.1371/journal.ppat.0020136.t001

of-the-flattest effect. The slope of the log regression (0.017 ± 0.033) was slightly, although non-significantly (*t*-test, $p = 0.622$), positive, suggesting that the competitive advantage of CSVd vanished as a consequence of the 2-fold larger mutational neutral neighborhood surrounding CChMVd's optimum genotype.

The Observations Cannot Be Explained by UVC-Induced Differences in Plant Physiology

It was necessary to exclude the possibility that the above observations were driven primarily by UVC-induced differences in plant responses to viroid infection (e.g., UVC light induction of SOS-like functions that disproportionately affected CSVd replication) rather than, as we hypothesized, determined by the competition dynamics between both viroids. To this end, we analyzed plants singly infected with each viroid that had been treated in exactly the same manner as the coinfected plants. On average, no compelling differences were found between samples taken after 4 wk and 6 wk (test of covariable: $F_{1,35} = 0.418$, $p = 0.522$), indicating that viroid concentrations were in steady state density after 4 wk, and, as expected, different for each viroid (test of viroid species factor: $F_{1,35} = 600.571$, $p < 0.001$). The UVC treatment negatively impacted the accumulation of both viroids. Indeed, treated plants carried, on average, 23.81% fewer viroid RNA molecules than the control plants (test of treatment factor: $F_{1,35} = 12.869$, $p = 0.001$). However, this negative effect of UVC light on viroid accumulation during single infections was the same for both viroids (test of the interaction term: $F_{1,35} = 2.245$, $p = 0.143$). Nevertheless, this is a negative result, and the objection can be raised that our experiment lacked sufficient power to reject the null hypothesis of no differential effect of UVC radiation on each viroid's accumulation. Statistical power reflects several factors, including sample size and the ratio of signal to noise. Computation of variance components [31] indicates that the error variance due to imprecision in measuring viroid concentration ($s^2 = 0.141$) only represents 5.98% of total variance. Thus, the negative result cannot be entirely due to noisy measurements. A second and more direct approach to the statistical power of the test of the interaction term is to compute the confidence interval for the *F* ratio test statistic and then estimate the significance level for its upper 95% limit (the worst-case value). According to Tukey's jackknife method [31], the 95% confidence interval for the test statistic was $-3.693 \leq F_{1,35} \leq 4.124$. Hence, in the worst case, the probability of accepting the null hypothesis of equal effects of UVC radiation on the accumulation of CSVd and CChMVd as actually being false is only $p = 0.050$. All in all, any change in plant physiology associated with the mutagenic treatment did not differentially impact the accumulation of each viroid. Therefore, we conclude that the outcome of the competition experiments run under mutagenic conditions is most likely due to the survival-of-the-flattest effect rather than to viroid-specific interactions with plant factors influenced by UVC irradiation. However, competition experiments in some cases may magnify differences in viral fitness that were undetectable when replication rate was the only measurable parameter (e.g., by one-step growth curves). As such, it may be possible that UVC induced changes in plant physiology that had a minor effect on CSVd replication and were undetectable with the power of our experiments; however, these changes became important only during competition against CChMVd. Although certainly possible, the above power analyses leave little room for this possibility.

Characterization of Genetic Variability

To better understand the effect of the mutagenic and control treatments on the genetic composition of CChMVd and CSVd quasispecies, we randomly picked three plants from each treatment after 6 wk and cloned and sequenced 20 molecules from each viroid per plant. First, we confirmed the mutagenic effect of UVC radiation. If UVC radiation increases genetic variability, then it is expected that the number of new haplotypes (i.e., those that were not detected in the coinfected plants prior to the mutagenic treatment) in the irradiated plants would be larger than in the non-irradiated plants. When this calculation was done for CSVd, the average frequency of new haplotypes across non-irradiated plants (Dataset S5) was 66.87% (i.e., approximately 1/3 of the haplotypes were already detected in the ancestral population), but increased to 92.32% in irradiated plants (Dataset S6) (i.e., only 7.68% of identified haplotypes were detected in the ancestral population). Therefore, there are 38.6% more new haplotypes in the irradiated plants than in

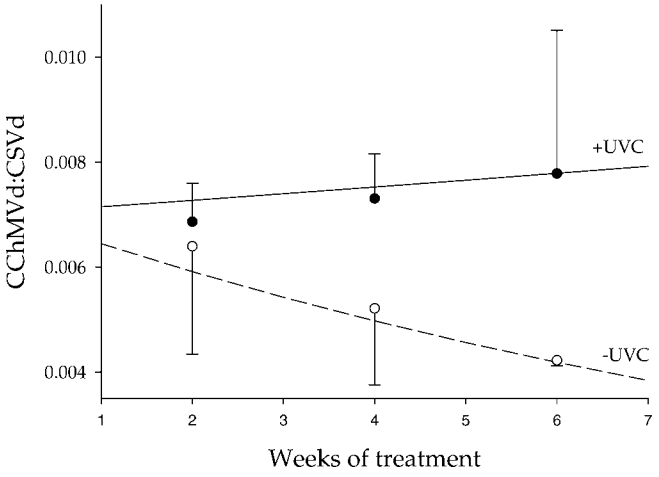

Figure 1. Competition Experiments among CChMVd and CSVd under Normal and Mutagenic Environmental Conditions

Black dots represent +UVC treatment while open dots represent control treatment. Each dot represents the median of the ratios estimated for multiple plants. Error bars represent the jackknife estimate of the standard error of the median. The lines represent the best fit to the non-linear model described in Materials and Methods.
doi:10.1371/journal.ppat.0020136.g001

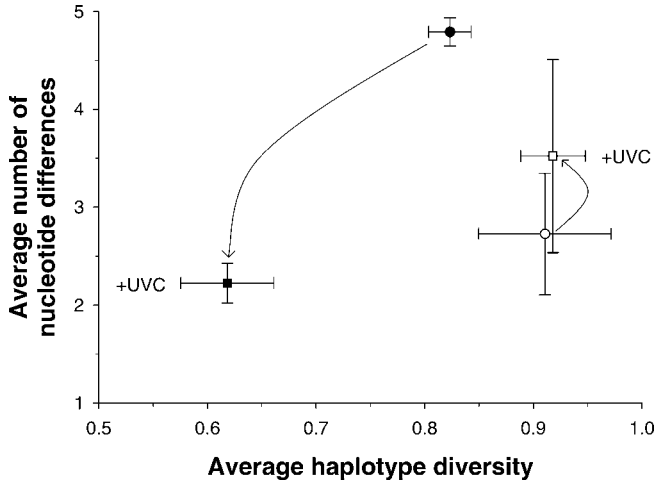

Figure 2. Characterization of the Genetic Diversity of the Competing Viroid Populations

Two measures of the genetic diversity (± SEM) of the CChMVd (open symbols) and CSVd (solid symbols) populations 6 wk after initiation of the competition experiments. Three plants were analyzed for each treatment (20 clones of each viroid per plant). Circles represent the averages from control plants and squares the averages from UVC-treated plants. Arrows indicate the direction of the UVC effect.
doi:10.1371/journal.ppat.0020136.g002

the control ones, the difference being statistically significant ($t_4 = 3.872$, $p = 0.018$). The picture for CChMVd is slightly different. None of the haplotypes present in the ancestral population was detected in the evolved ones; thus, both UVC-treated (Dataset S3) and non-treated (Dataset S2) CChMVd populations were constituted by newly created haplotypes. This is not surprising given the already high level of diversity in CChMVd prior to the competition experiment.

Second, we analyzed the genetic diversity present in each plant. To do so, the haplotype diversity and the average number of nucleotide differences were computed. Diversity data from each viroid were compared using model II nested analysis of variance in which the "plant" factor was nested within "treatment". Both factors were treated as random factors. Figure 2 shows the averages of these two measures across plants. On the one hand, the survival-of-the-flattest effect predicts that a robust organism replicating under mutagenic conditions would increase its genetic variability without noticeably affecting its fitness. In other words, a larger genetic variability is expected for CChMVd under UVC than under control conditions. Although the differences were not statistically significant, the change in the data goes in the expected direction (Figure 2). CChMVd quasispecies replicating under UVC contained, on average, 0.8% more haplotypes and 30.3% more nucleotide differences than CChMVd quasispecies replicating under non-mutagenic conditions. On the other hand, the hypothesis predicts the opposite effect for a non-robust organism, such that the extrinsic increase in mutation rate would produce very low-quality genotypes (including lethal ones) that compete poorly against robust organisms and therefore would be quickly eliminated from the population. Only those molecules preserving a sequence close to the wild-type, which rapidly becomes a minority, will be capable of surviving. Hence, a reduction in the amount of viable (and therefore detectable) genetic variation within CSVd quasispecies is expected under UVC conditions. Indeed, this is the pattern observed for CSVd (Figure 2). On average, CSVd quasispecies that evolved at a high mutation rate contained 24.9% fewer haplotypes than control populations (test of the UVC effect; $p = 0.009$) and with 30.3% fewer nucleotide differences ($p < 0.001$).

Simulation Analysis and Results

To support the above interpretation, we simulated two populations of digital viroids (bit strings) replicating, mutating, and competing on a given landscape at given mutation rates. The fitness of each competing population was modeled by a multiplicative decaying function $f(k)$ of the number of mutations k. The sharpness or flatness of the landscape was controlled by a single parameter s (small for flat peaks and large for sharp peaks). The previously mentioned non-viability for highly mutated CSVd genomes was incorporated by the cutoff condition $f(k) = 0$ if $k > k_c$. Because little is known about the exact parameters that might fit the experimental results, we performed a search of parameter combinations such that they were consistent with the experimental observations. The algorithm systematically searched the parameter space defined by $\{s_{\mathrm{CSVd}}, s_{\mathrm{CChMVd}}, \mu, \mu^{\mathrm{UVC}}, k_c\}$, where μ and μ^{UVC} are the mutation rates under control and UVC conditions, respectively. The target is defined in terms of minimizing the distance between the number of nucleotide differences found in the *in planta* experiments and those generated by the in silico model runs. The size ν of the bit strings was fixed to $\nu = 64$ and initial populations of $N = 2{,}000$ bit strings of each class were used. After 40 generations, 20 bit strings of each class were randomly sampled and the average number of differences (the Hamming distance, D_H) calculated over five independent runs. If the survival-of-the-flattest effect is at work, the average fitness of the digital-CSVd population should be smaller than the average fitness of the digital-CChMVd

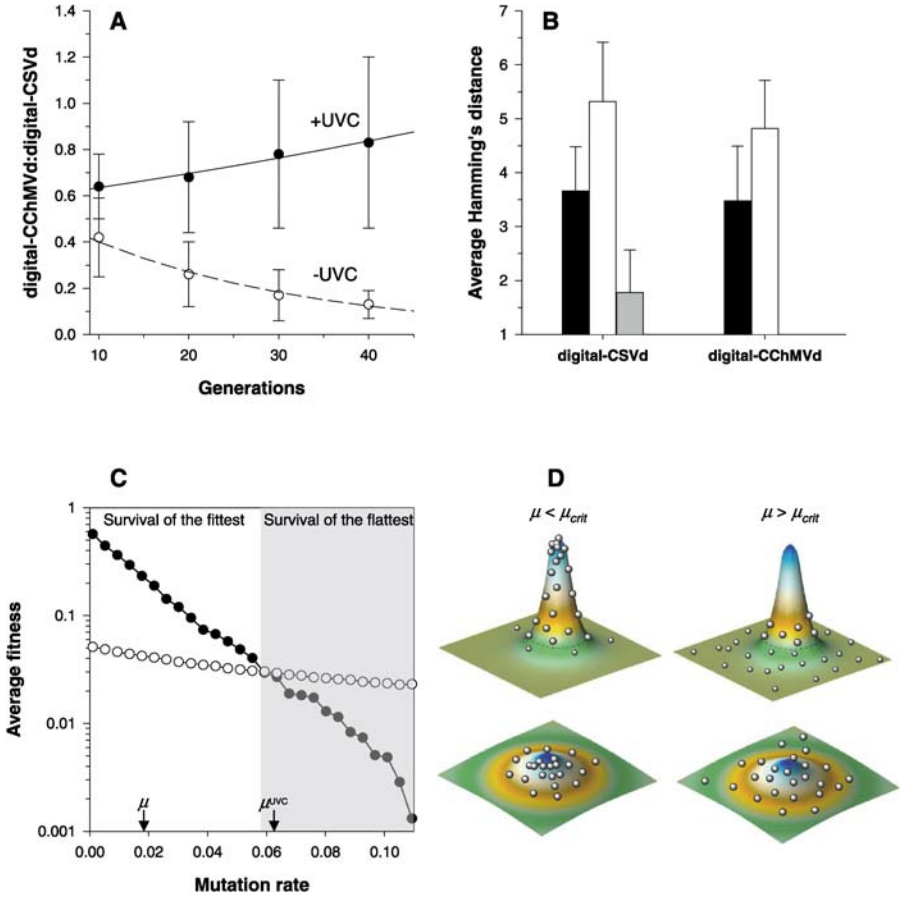

Figure 3. Results from the Simulation Model of Competing Bit String Populations

The best solution obtained by searching over parameter space is shown ($s_{CSVd} = 0.33$, $s_{CChMVd} = 0.05$, $\mu = 0.016$, $\mu^{UVC} = 0.063$, and $k_c = 3$).

(A) Population dynamics under control and UVC conditions, sampled over five different replicates over 40 generations.

(B) Average Hamming distance $D_H = \sum_{k=1}^{\nu} |S_{ik} - S_{jk}|$ among sampled digital viroids (± SEM). Solid bars correspond to the control conditions, open bars to UVC conditions, and gray bars to UVC conditions after exclusion of the 66.5% CSVd lethal genotypes from the computations.

(C) The survival-of-the-flattest effect is shown here using the two populations that evolved separately with increasing mutation rates. The average fitness for each population is plotted against mutation rate. Using the above s_{CSVd}, s_{CChMVd}, and k_c values, the mutation rate was allowed to vary from $\mu = 0.001$ to $\mu = 0.15$. At a given critical mutation rate (here $\mu_{crit} = 0.059$), the average fitness of digital-CSVd (solid dots and continuous line) starts to decay below the one shown by digital-CChMVd (open dots and dashed line). The domain where the flattest wins over the fittest is indicated as a gray area.

(D) Shows a cartoon interpretation of the observed effect of high mutation rate on average fitness and variability.

doi:10.1371/journal.ppat.0020136.g003

population after some critical mutation rate, μ_{crit}, is exceeded. Figure 3 summarizes the results of these simulations. The outcome of the in silico competition experiments is shown in Figure 3A for the best-fitting combination of parameters (see the Figure 3 legend for estimated values). Results perfectly match those observed *in planta* for a 4-fold increase in mutation rate and a mutational load cutoff for CSVd of three mutations (regression of observed to simulated data: $R^2 = 0.995$, $p = 0.003$).

Figure 3B illustrates the changes in genetic diversity induced by this 4-fold increase in mutation rate for both digital viroids. In silico results are consistent with the *in planta* observations: digital-CChMVd populations were 38.5% more diverse after the mutation rate increase. The situation for digital-CSVd populations replicating at a high mutation rate is a bit more complex and depends on whether or not lethal genotypes are taken into consideration when computing the average D_H between digital genomes. Indeed, the lethality fraction (i.e., the number of genomes carrying more than three substitutions) was as large as 66.5%. When lethal genotypes were incorporated into the computation, digital-CSVd population diversity also increased to 45.4%. However, if lethals were not considered for calculating the average D_H, digital-CSVd populations were 51.4% less variable than non-mutagenized digital-CSVd populations, which is in agreement with the *in planta* observations. Thus, we conclude that the apparent reduction in genetic diversity experimentally observed for CSVd populations competing at a high mutation rate is entirely explained by the existence of a large fraction of lethal genotypes that bring about the reversal of fortune in the survival-of-the-flattest effect. In turn, these lethal genotypes cannot be detected by cloning and sequencing methods in the in vivo experiments.

As predicted from the survival-of-the-flattest hypothesis, a crossing between average fitnesses takes place with increasing

mutation rates; Figure 3C depicts the optimal solution found with the parameter search algorithm.

Finally, the qualitative interpretation of our results is displayed in Figure 3D. Below the critical mutation rate, the two populations appear close to their corresponding peaks. At high mutation rates, whereas the flattest population spreads farther across its fitness landscape, the fittest population only spreads until it reaches the mutational cutoff (dashed line) and surviving strings are scattered around it (upper row). Those mutant sequences having a larger number of mutations than the cutoff are unviable (small white balls).

Concluding Remarks

We have shown that under high mutation rate conditions, a slowly replicating organism can easily displace a faster replicating one, provided that the former is supported by a neutral neighborhood capable of buffering the increasing mutational load; in demonstrating this we have thus provided empirical evidence for the survival of the flattest effect in a biological system [6–8]. In this case, a 20-fold difference in replication efficiency was overcome by only a 2-fold increase in the neutral neighborhood. This observation also supports the existence of a tradeoff between replication rate and mutational robustness [4,6]. Finally, these findings also clarify the importance of the mutational swarm, as described by the quasispecies model [1–4], for the evolution of RNA replicons. In recent years doubts have been expressed about the applicability of the quasispecies model to viral evolution [32,33]. Detractors have argued that evidence supporting the quasispecies model was weak and that clear evidence for the action of selection on mutational robustness or for a faster replicator being outcompeted by a slower one was missing. Here, we have provided such evidence for subviral plant pathogens.

Materials and Methods

RNA purification, quantification, and sequencing. Tissue from viroid-infected chrysanthemums was homogenized, and viroid RNA preparations were obtained by chromatography on nonionic cellulose [34]. RNA preparations were separated by denaturing PAGE in 5% gels containing 8 M urea in TBE buffer [35], electroblotted to nylon membranes, and hybridized with viroid-specific ^{32}P-labeled riboprobes at 70 °C in the presence of 50% formamide [36]. Hybridization signals were quantified using a Fuji BAS1500 bioimage analyzer (http://www.fujifilm.com). For viroid cloning and sequencing, viroid RNAs were RT-PCR-amplified with SuperScript III reverse transcriptase (Invitrogen, http://www.invitrogen.com) and Pfu DNA polymerase (Stratagene, http://www.stratagene.com) by using CChMVd-specific (complementary: 5′-GACCTCTTGGGGGTTT-CAAACCC-3′ and homologous: 5′-GGCACCTGATGTCGGTGTCCT-GATG-3′) and CSVd-specific (complementary: 5′-GGGGATCCCTGAAGGACTTCT-3′ and homologous: 5′-GGGGAAACCTGGAGGAAG-3′) primers. The amplified cDNAs were ligated into a SmaI-opened pUC18 plasmid and used to transform *Escherichia coli* DH5α. The cDNAs from the resulting recombinant plasmids were sequenced with an ABI Prism 3100 Genetic Analyzer (Applied Biosystems, http://www.appliedbiosystems.com). All sequences data are provided in MSF format in Datasets S1–S6. Dataset S1 contains the ancestral sequences for CChMVd, whereas Datasets S2 and S3 contain CChMVd sequences from control plants and UVC-irradiated plants, respectively. Dataset S4 contains the ancestral sequences for CSVd, and Datasets S5 and S6 the CSVd sequences from control and UVC-irradiated plants, respectively.

Effect of UVC radiation on the accumulation of each viroid. To assess whether the mutagenic treatment differentially affected the accumulation of each viroid species, 20 chrysanthemums were singly inoculated with CSVd and 20 more with CChMVd. Half of the plants were placed at mutagenic conditions and half were kept under control conditions. Then, 4 wk and 6 wk after inoculation, tissue was homogenized and the concentration of each viroid quantified by Northern blot analysis as described above. Upon log transformation, the data were analyzed by means of a model II two-way analysis of variance using time as covariable [31].

In silico mutational robustness analysis. For each viroid, we measured mutational neutrality, which is the fraction of all possible point mutations that do not disturb the folding of the unmutated RNA molecule. A molecule of length l will have $4l$ one-error mutants (including one-nucleotide deletions). For each one of the $4l$ mutants, we numerically evaluated its minimum free energy secondary structure and compared it with that of the unmutated genotype. Folding and comparison among structures was done using ViennaRNA package version 1.4 [20].

Statistical analysis of the competition data. For each plant sample, the ratio between CChMVd and CSVd was estimated by Northern blot hybridization analysis using equal counts of specific ^{32}P-labeled riboprobes. Then, for each time point shown in Figure 1, we computed the median ratio (R_t) instead of the mean to minimize the effect of outliers. The standard error of the median was obtained by Tukey's jackknife method [31]. Then, medians were fitted to the non-linear model $\ln R_t = \ln R_0 + (a + \delta_a M)t$, where a represents the common slope and δ_a accounts for differences in the treatment effect on the slope ($M = 0$ for control treatment and $M = 1$ for mutagenic treatment). A $\delta_a \neq 0$ value indicates a significant treatment effect. In Figure 1, the fit of the model was highly significant ($R^2 = 0.9541$, $p < 0.001$). The least squares estimates of the parameters were $\ln R_0 = -4.958 \pm 0.077$ (t-test, $p < 0.001$), $a = -0.086 \pm 0.019$ (t-test, $p = 0.011$), and $\delta_a = 0.104 \pm 0.014$ (t-test, $p = 0.002$).

In silico competition model. The population of competing viroids was simulated using a binary bit string model [37], where each digital viroid was represented by a binary string $\boldsymbol{S}_i = (S_{i1}, \ldots, S_{i\nu})$, where $S_{ij} \in \{0, 1\}$, ν is the genome length, and $i = 1, \ldots, N$, N being the maximum population size. The population started with a small sample of size $N_0 < N$ of each competing viroid. Initial populations were sampled from two independent populations evolved to the stationary state under control conditions. The other $N - 2N_0$ strings were empty. The fitness of a string S_i, indicated as $f(S_i)$, is a decreasing function of the number of mutations with respect to the master sequence, defined as the all-ones string. For a sequence at a Hamming distance of k mutations from the master sequence, fitness was computed using a multiplicative landscape [38]:

$$f(S_i) = \frac{(1-s)^k}{\sum_{j=0}^{\nu}(1-s)^j}, \tag{1}$$

where $k = \nu - \sum_{l=1}^{\nu} S_{il}$. The parameter s weights the relative decrease of fitness associated with mutations (i.e., the peak steepness). Digital-CSVd populations are expected to have a sharp peak, with a large s_{CSVd} value and thus fitness rapidly decaying until reaching the cutoff k_c, beyond which molecules are unable to replicate:

$$f(S_i) = \frac{(1-s)^k}{\sum_{j=0}^{k_c}(1-s)^j} \tag{2}$$

if $k < k_c$ and zero otherwise. Digital-CChMVd populations inhabit a flat peak with $s_{\mathrm{CChMVd}} < s_{\mathrm{CSVd}}$; thus, mutations have a much smaller effect on fitness. Each digital viroid can be degraded and removed with probability $\delta = 0.01$. Each generation involves N independent individual updates in which each digital viroid is chosen to replicate with probability $f(S_i)$ and each bit can mutate with probability μ. Specifically, at each round of replication, every bit S_{ij} in the newborn string can mutate to $1 - S_{ij}$ with probability μ. The presence of a survival-of-the-flattest effect can be predicted by looking at the equilibrium distributions of each competing population under varying mutation rates [8,39]. Specifically, for a given parameter combination, the average fitness, $\langle f(s, \mu)\rangle$, of our digital populations will be

$$\langle f(s,\mu)\rangle = \frac{1}{N}\sum_{k=1}^{N} P(S_k) f(S_k) = \frac{1}{N}\sum_{k=1}^{N} P(S_k)\frac{(1-s)^k}{\sum_j (1-s)^j}, \tag{3}$$

where $P(S_k)$ represents the frequency of genotype S_k in the population. If there is a fitness change at some given mutation rate, μ_{crit}, where the sign of $\langle f(s_1,\mu)\rangle - \langle f(s_2,\mu)\rangle$ changes from positive (fittest

wins) to negative (flattest wins), then a survival of the flattest scenario should be observed as this critical mutation rate is crossed. This criterion was used in searching for candidate solutions that consistently matched the experimental observations with the theoretical prediction.

Supporting Information

Dataset S1. CChMVd Ancestral Sequences

Found at doi:10.1371/journal.ppat.0020136.sd001 (7 KB TXT).

Dataset S2. CChMVd Sequences from Control Plants

Found at doi:10.1371/journal.ppat.0020136.sd002 (25 KB TXT).

Dataset S3. CChMVd Sequences from UVC-Treated Plants

Found at doi:10.1371/journal.ppat.0020136.sd003 (20 KB TXT).

Dataset S4. CSVd Ancestral Sequences

Found at doi:10.1371/journal.ppat.0020136.sd004 (9 KB TXT).

Dataset S5. CSVd Sequences from Control Plants

Found at doi:10.1371/journal.ppat.0020136.sd005 (23 KB TXT).

Dataset S6. CSVd Sequences from UVC-Treated Plants

Found at doi:10.1371/journal.ppat.0020136.sd006 (23 KB TXT).

Acknowledgments

We thank F. de la Iglesia and V. Moncholí for technical assistance; S. Gago and A. E. Martínez de Alba for sharing infected materials; R. Flores, A. Munteanu, C. Rodríguez-Caso, R. Sanjuán, and C. O. Wilke for discussions; and G. Velicer for improving our English.

Author contributions. JAD and SFE conceived and designed the experiments. FMC, JAD, and SFE performed the experiments. RVS and SFE analyzed the data and wrote the paper.

Funding. This work was supported by grants from the Ministerio de Educación y Ciencia–Fondo Europeo de Desarrollo Regional (FEDER) and the Generalitat Valenciana (SFE and JAD), the European Molecular Biology Organization Young Investigator Programme (EMBO YIP) (SFE), and the European Union Future and Emerging Technologies (FET) project Programmable Artificial Cell Evolution (PACE) (RVS).

Competing interests. The authors have declared that no competing interests exist.

References

1. Eigen M (1971) Selforganization of matter and the evolution of biological macromolecules. Naturwissenschaften 58: 465–523.
2. Eigen M, McCaskill J, Schuster P (1989) The molecular quasispecies. Adv Chem Phys 75: 149–263.
3. Nowak MA (1992) What is a quasispecies? Trends Ecol Evol 7: 118–121.
4. Schuster P, Swetina J (1988) Stationary mutant distributions and evolutionary optimization. Bull Math Biol 50: 635–660.
5. van Nimwegen E, Crutchfield JP, Huynen M (1999) Neutral evolution of mutational robustness. Proc Natl Acad Sci U S A 96: 9176–9720.
6. Wilke CO (2001) Adaptive evolution on neutral networks. Bull Math Biol 63: 715–730.
7. Wilke CO, Wang JL, Ofria C, Lenski RE, Adami C (2001) Evolution of digital organisms at high mutation rate leads to survival of the flattest. Nature 412: 331–333.
8. Wilke CO, Adami C (2003) Evolution of mutational robustness. Mut Res 522: 3–11.
9. Wilke CO (2001) Selection for fitness versus selection for robustness in RNA secondary structure folding. Evolution 55: 2412–2420.
10. Flores R, Hernández C, Martínez de Alba AE, Daròs JA, di Serio F (2005) Viroids and viroid–host interactions. Annu Rev Phytopathol 43: 117–139.
11. Daròs JA, Elena SF, Flores R (2006) Viroids: An Ariadne's thread into the RNA labyrinth. EMBO Reports 7: 593–598.
12. Diener TO, Lawson RH (1973) Chrysanthemum stunt: A viroid disease. Virology 51: 94–101.
13. Navarro B, Flores R (1997) Chrysanthemum chlorotic mottle viroid: Unusual structural properties of a subgroup of self-cleaving viroids with hammerhead ribozymes. Proc Natl Acad Sci U S A 94: 11262–11267.
14. Bonfiglioli RG, McFadden GI, Symons RH (1994) In situ hybridization localizes avocado sunblotch viroid on chloroplast thylakoid membranes and coconut cadang cadang viroid in the nucleus. Plant J 6: 99–103.
15. Bonfiglioli RG, Webb DR, Symons RH (1996) Tissue and intra-cellular distribution of coconut cadang cadang viroid and citrus exocortis viroid determined by in situ hybridization and confocal laser scanning and transmission electron microscopy. Plant J 9: 457–465.
16. Bussière F, Lehoux J, Thompson DA, Skrzeczkowski LJ, Perreult J (1999) Subcellular location and rolling circle replication of peach latent mosaic viroid: Hallmarks of group A viroids. J Virol 73: 6353–6360.
17. Wagner A, Stadler PF (1999) Viral RNA and evolved mutational robustness. J Exp Zool 285: 119–127.
18. Ancel LW, Fontana W (2000) Plasticity, evolvability, and modularity in RNA. J Exp Zool 288: 242–283.
19. Meyers LA, Lee JF, Cowperthwaite M, Ellington AD (2004) The robustness of naturally and artificially selected nucleic acid secondary structures. J Mol Evol 58: 681–691.
20. Hofacker IL, Fontana W, Stadler PF, Bonhoeffer S, Tacker M, Schuster P (1994) Fast folding and comparison of RNA secondary structures. Monatsh Chem 125: 167–188.
21. Govier DA, Kleczkowski A (1970) Inactivation by ultraviolet radiation at different wavelengths of the RNA isolated from potato virus X. Photochem Photobiol 12: 345–353.
22. Dubinin NP, Zasukhina GD, Nesmashova VA, Lvova GN (1975) Spontaneous and induced mutagenesis in western equine encephalomyelitis virus in chick embryo cells with different repair activity. Proc Natl Acad Sci U S A 72: 386–388.
23. Saika S, Kidokoro M, Kubonoya H, Ito K, Ohkawa T, Aoki A, Nagata N, Suzuki K (2006) Development and biological properties of a new live attenuated mumps vaccine. Comp Immunol Microbiol Infect Dis 29: 89–99.
24. Diener TO, Schneider IR, Smith DR (1974) Potato spindle tuber viroid. XI. A comparison of the ultraviolet light sensitivities of PSTV, tobacco ringspot virus, and its satellite. Virology 57: 577–581.
25. Remsen JF, Miller N, Cerutti PA (1970) Photohydration of uridine in the RNA of coliphage R17. II. The relationship between ultraviolet inactivation and uridine photohydration. Proc Natl Acad Sci U S A 65: 460–466.
26. Zhirnov OV, Wollenzien P (2003) Action spectra for UV-light induced RNA–RNA crosslinking in 16S ribosomal RNA in the ribosome. Photochem Photobiol Sci 2: 688–693.
27. Grossman L (1962) The effects of ultraviolet-irradiated polyuridylic acid in cell-free protein synthesis in *E. coli*. Proc Natl Acad Sci U S A 48: 1609–1614.
28. Fraga CG, Shigenaga MK, Park JW, Degan P, Ames BN (1990) Oxidative damage to DNA during aging: 8-hydroxy-2′-deoxyguanosine in rat organ DNA and urine. Proc Natl Acad Sci U S A 87: 4533–4537.
29. Branch AD, Benenfeld BJ, Robertson HD (1985) Ultraviolet light-induced crosslinking reveals a unique region of local tertiary structure in potato spindle tuber viroid and HeLa 5S RNA. Proc Natl Acad Sci U S A 82: 6590–6594.
30. Hernández C, di Serio F, Ambrós S, Daròs JA, Flores R (2006) An element of the tertiary strucutre of peach latent mosaic viroid RNA revealed by UV irradiation. J Virol 80: 9336–9340.
31. Sokal RR, Rohlf FJ (1995) Biometry. 3rd edition. New York: Freeman. 880 p.
32. Jenkins GM, Worobey M, Woelk CH, Holmes EC (2001) Evidence for the non-quasispecies evolution of RNA viruses. Mol Biol Evol 18: 987–994.
33. Holmes EC, Moya A (2002) Is the quasispecies concept relevant to RNA viruses? J Virol 76: 460–465.
34. Pallás V, Navarro A, Flores R (1987) Isolation of a viroid-like RNA from hop different from hop stunt viroid. J Gen Virol 68: 3201–3205.
35. Sambrook J, Russell DW (2001) Molecular cloning: A laboratory manual. 3rd edition. Cold Spring Harbor (New York): Cold Spring Harbor Laboratory Press. 999 p.
36. Daròs JA, Marcos JF, Hernández C, Flores R (1994) Replication of avocado sunblotch viroid: Evidence for a symmetric pathway with two rolling circles and hammerhead ribozyme processing. Proc Natl Acad Sci U S A 91: 12813–12817.
37. Solé RV, Ferrer R, González-García I, Quer J, Domingo E (1998) Red queen dynamics, competition and critical points in a model of RNA virus quasispecies. J Theor Biol 198: 47–59.
38. Krakauer DC, Plotkin JB (2002) Redundancy, antiredundancy, and the robustness of genomes. Proc Natl Acad Sci U S A 99: 1405–1409.
39. Bull JJ, Ancel Meyer L, Lachman M (2005) Quasispecies made simple. PLoS Comput Biol 1: e61. doi:10.1371/journal.pcbi.0010061.